

The 3.4 micron absorption feature towards three obscured active galactic nuclei

M. Imanishi ^{1,2}

¹ National Astronomical Observatory, Mitaka, Tokyo 181-8588, Japan

² Institute for Astronomy, University of Hawaii, 2680 Woodlawn Drive, Honolulu, Hawaii 96822, USA

ABSTRACT

The results of 3–4 μm spectroscopy towards the nuclei of NGC 3094, NGC 7172, and NGC 7479 are reported. In ground-based 8–13 μm spectra, all the sources have strong absorption-like features at $\sim 10 \mu\text{m}$, but they do not have detectable polycyclic aromatic hydrocarbon (PAH) emission features. The 3.4 μm carbonaceous dust absorption features are detected towards all nuclei. NGC 3094 shows a detectable 3.3 μm PAH emission feature, while NGC 7172 and NGC 7479 do not. Nuclear emission whose spectrum shows dust absorption features but no PAH emission features is thought to be dominated by highly obscured active galactic nuclei (AGNs) activity. For NGC 7172, NGC 7479, and three other such nuclei in the literature, we investigate the optical depth ratios between the 3.4 μm carbonaceous dust and 9.7 μm silicate dust absorption ($\tau_{3.4}/\tau_{9.7}$). The $\tau_{3.4}/\tau_{9.7}$ ratios towards three highly obscured AGNs with face-on host galaxies are systematically larger than the ratios in the Galactic diffuse interstellar medium or the ratios for two highly obscured AGNs with edge-on host galaxies. We suggest that the larger ratios can be explained if the obscuring dust is so close to the central AGNs that a temperature gradient occurs in it. If this idea is correct, our results may provide spectroscopic evidence for the presence of the putative “dusty tori” in the close vicinity of AGNs.

Key words: galaxies: active — galaxies: nuclei — galaxies: individual: NGC 3094, NGC 7172, and NGC 7479 — infrared: galaxies

1 INTRODUCTION

This is the second paper in a series that investigates the 3.4 μm carbonaceous dust absorption feature in sources that show a strong absorption-like feature at $\sim 10 \mu\text{m}$ but no detectable polycyclic aromatic hydrocarbon (PAH) emission features in ground-based 8–13 μm (i.e., whole the N -band) spectra. The first paper discusses NGC 5506 (Imanishi 2000). Roche et al. (1991) performed extensive ground-based 8–13 μm spectroscopy of the nuclei of nearby active galaxies (mostly $z < 0.05$), and classified them into the following three groups: (1) those dominated by the family of emission features from small molecules called PAHs (20–40 carbon atoms per molecule; Allamandola, Tielens & Barker 1989), (2) those with a featureless continuum, and (3) those that display an absorption-like feature at $\sim 10 \mu\text{m}$. Each group of sources is regarded as, respectively, (1) those powered by star-forming activity, (2) those powered by unobscured active galactic nuclei (AGNs) activity, and (3) those powered by obscured AGN activity, for which the silicate dust absorption feature at $\sim 9.7 \mu\text{m}$ is expected to be present. Sources

in the third group, in particular those with a strong silicate dust absorption feature, are expected to be highly obscured AGNs, and thus can be used to investigate the properties of the intervening medium along our line-of-sight through the study of infrared absorption features.

However, the attribution of the strong absorption-like feature at $\sim 10 \mu\text{m}$ detected in many ground-based 8–13 μm spectra to the 9.7 μm silicate dust absorption has been questioned based on the *Infrared Space Observatory (ISO)* spectra (Clavel et al. 1999; Genzel et al. 1998). Strong PAH emission at 7.7 μm from star-forming activity and continuum flux that increases with wavelength could produce an apparent strong absorption-like feature at $\sim 10 \mu\text{m}$. One can attempt to estimate the strength of the 7.7 μm PAH emission based on the observed flux of the PAH emission at 8.6 μm and 11.3 μm in ground-based 8–13 μm spectra (Dudley 1999) by assuming that the 7.7 μm PAH emission is weak in sources with no detectable 8.6 μm and 11.3 μm PAH emission. However, this estimate could sometimes be uncertain (Rigopoulou et al. 1999).

Spectroscopy at 3–4 μm can be a powerful method for

2 *Imanishi*

finding a highly obscured AGN, not only because the effect of extinction is small at 3–4 μm , but also because there exist emission and absorption features for distinguishing between highly obscured AGN and star-forming activities. If a source is powered by star-forming activity, PAH emission features should be detected at 3.3 μm and sometimes at 3.4 μm (Tokunaga et al. 1991). If a source is powered by obscured AGN activity, a 3.4 μm absorption feature associated with carbonaceous dust grains (Pendleton et al. 1994) should be detected. An advantage of a ground-based 3–4 μm spectrum over a ground-based 8–13 μm spectrum is that there is no serious uncertainty in determining a continuum level for the former. This is because both the long and short wavelength sides of the features at 3.3–3.4 μm are observable in the *L*-band atmospheric window (2.8–4.2 μm) for a nearby ($z < 0.18$) source. Furthermore, if both (less obscured) star-forming activity and obscured AGN activity are associated in a galaxy, the 3.4 μm absorption feature is suppressed because the observed spectrum is dominated by emission from the less obscured star-forming activity and/or the emission at 3.4 μm by PAHs could veil the absorption feature. Therefore, sources with a strong 3.4 μm absorption feature that also lacks a PAH emission feature are the ones most likely to be highly obscured AGNs with little star-forming activity. Unfortunately, high-quality 3–4 μm spectra for sources with a strong absorption-like feature at $\sim 10 \mu\text{m}$ but no detectable PAH emission features in ground-based 8–13 μm spectra are available only for a few objects. Examples include NGC 1068 (Bridger, Wright & Geballe 1994; Imanishi et al. 1997), IRAS 08572+3915 (Pendleton 1996; Wright et al. 1996) and NGC 5506 (Imanishi 2000).

Here, we have performed 3–4 μm spectroscopy on three such sources, with the aim of detecting the 3.4 μm carbonaceous dust absorption feature.

2 TARGETS

2.1 NGC 3094

NGC 3094 ($z = 0.008$) is a spiral galaxy (Huang et al. 1996). Its nuclear optical spectrum is classified as an AGN-type (Armus, Heckman & Miley 1989). A ground-based 8–13 μm spectrum taken with a 3''.8 aperture displays a strong absorption-like feature at $\sim 10 \mu\text{m}$, but no detectable PAH emission features (Roche et al. 1991).

2.2 NGC 7172

NGC 7172 ($z = 0.009$) is an edge-on galaxy of type S0–Sa with a clear equatorial dust lane along roughly the east–west direction (Anupama et al. 1995). An obscured AGN was found in the hard X-ray (Piccinotti et al. 1982). A ground-based 8–13 μm spectrum taken with a 4''.2 aperture displays a strong absorption-like feature at $\sim 10 \mu\text{m}$, but no detectable PAH emission features (Roche et al. 1991).

2.3 NGC 7479

NGC 7479 ($z = 0.008$) is a spiral galaxy of type SBbc (Sandage & Tammann 1987). Its grand design spiral arms are clearly seen in the Digitized Sky Survey image, and

therefore the viewing direction towards the galaxy is estimated to be far from edge-on (Ma, Peng & Gu 1998). Recent high-quality optical to near-infrared spectra suggest the presence of an obscured AGN in NGC 7479 (Ho, Filippenko & Sargent 1997; Larkin et al. 1998). A ground-based 8–13 μm spectrum taken with a 4''.3 aperture displays a strong absorption-like feature at $\sim 10 \mu\text{m}$, but no detectable PAH emission features (Roche et al. 1991).

3 OBSERVATION AND DATA ANALYSIS

The 3–4 μm spectra towards NGC 3094, NGC 7172, and NGC 7479 were obtained at the 3.8-m United Kingdom Infrared Telescope (UKIRT) on Mauna Kea, Hawaii, using the cooled grating spectrometer (CGS4; Mountain et al. 1990). An observing log is summarized in Table 1. The sky was photometric throughout the observations. The detector was a 256×256 InSb array. A 40 l mm^{-1} grating with a 2 pixel wide slit ($= 1''.2$) was used.

Spectra were obtained towards the flux peak at $\sim 3.5 \mu\text{m}$. The slit position angles were set along the east–west direction for NGC 3094, and along the north–south direction for NGC 7172 and NGC 7479. A standard nodding technique along the slit direction with an amplitude of 11''.6 was employed to subtract the signal from the sky. The air masses during the observations and total on-source integration time are summarized in Table 1. Standard stars (Table 1) were observed with almost the same air masses as the target objects to correct for the transmission of Earth’s atmosphere. The main features in the spectra to be investigated were the 3.3 μm PAH emission and the 3.4 μm carbonaceous dust absorption features. Type-A rather than type-G stars were chosen as standard stars, in order to avoid possible small effects of stellar photospheric OH absorption at 3.0–3.6 μm in late-type stars (Smith, Sellgren & Brooke 1993).

Standard data analysis procedures were employed using IRAF^{*}. After the obtained frames were bias subtracted, they were divided by a flat image. The spectra of the targets and the standard stars were extracted using an optimal extraction algorithm. Wavelength calibration was performed using a Krypton or Argon lamp. The signals of the targets were divided by those of the standard stars and then multiplied by the spectrum of the blackbody with a temperature corresponding to individual standard stars (Table 1) to obtain the final spectra.

As a consequence of selecting type-A stars as standard stars, the resulting spectra are affected by strong stellar absorption features at 3.30 μm ($\text{Pf}\delta$) and at 3.74 μm ($\text{Pf}\gamma$). Since all targets are nearby, the (relatively narrow) Pf emission lines are affected by these absorption features, and therefore will not be discussed. When making the final spectra, the data at 3.31–3.32 μm have been removed, because the signals there are extremely small due to the strong methane absorption by Earth’s atmosphere. Since the data at 3.45–3.46 μm and 3.49–3.50 μm for NGC 7172 and NGC 7479 are affected by large noise levels that are difficult to

^{*} IRAF is distributed by the National Optical Astronomy Observatories, which are operated by the Association of Universities for Research in Astronomy, Inc. (AURA), under cooperative agreement with the National Science Foundation.

correct for completely, these data points have also been removed. Since the 3.3 μm PAH emission and the 3.4 μm carbonaceous dust absorption features have broad spectral profiles, their discussion is not seriously affected by the removal of these data points.

4 RESULTS

4.1 NGC 3094

A flux-calibrated spectrum of NGC 3094 is shown in Fig. 1. Our data give an L -band magnitude of 8.4 mag ($1''.2 \times 5''$ aperture), which is almost consistent to the photometric magnitude at L' measured with a $5''$ aperture (Dudley 1998; $L' = 129.8$ mJy or 8.2 mag).

In Fig. 1, a broad absorption-like feature is recognizable at ~ 3.35 – $3.55 \mu\text{m}$. We interpret the feature as the 3.4 μm carbonaceous dust absorption. In the Galaxy, the wavelength range of the 3.4 μm carbonaceous dust absorption feature is 3.33 – $3.55 \mu\text{m}$ in the rest-frame (Pendleton et al. 1994), which corresponds to 3.36 – $3.58 \mu\text{m}$ at the redshift of $z = 0.008$. The data points at $>3.58 \mu\text{m}$ are therefore not affected by this absorption feature. To avoid possible contamination by the $\text{Pf}\gamma$ emission line of NGC 3094, the data points at 3.58 – $3.72 \mu\text{m}$ are regarded as the continuum level on the long wavelength side of the absorption feature. On the short wavelength side of the absorption feature, the data points at $<3.26 \mu\text{m}$ are regarded as the continuum, because they are affected neither by the possible 3.3 μm PAH emission feature (3.25 – $3.35 \mu\text{m}$ in the rest-frame; Tokunaga et al. 1991) nor by the $\text{Pf}\delta$ emission line. The best linear fit to the data points at $<3.26 \mu\text{m}$ and at 3.58 – $3.72 \mu\text{m}$ is adopted as the continuum line for the 3.4 μm carbonaceous dust absorption feature. The adopted continuum level is displayed in Fig. 1 as a solid line. The resulting optical depth relative to this continuum level is $\tau_{3.4} \sim 0.04$ near the absorption peak. There may be some uncertainties in determining the continuum level. We also tried to determine the continuum level by varying the wavelength range slightly, and the resulting values for $\tau_{3.4}$ were within 10% of the value derived above for any reasonable continuum levels adopted.

In Fig. 1, a broad emission-like feature is found at $\sim 3.3 \mu\text{m}$. This feature is interpreted as the 3.3 μm PAH emission. Its rest-frame equivalent width is estimated to be $3.5 \pm 0.2 \times 10^{-3} \mu\text{m}$.

4.2 NGC 7172

A flux-calibrated spectrum of NGC 7172 is shown in Fig. 2. Our data give an L -band magnitude of 9.1 mag ($1''.2 \times 5''$ aperture), which is fainter than the values of 8.0–9.0 mag measured with $5''$ – $8''$ apertures (Sharples et al. 1984; Glass & Moorwood 1985; Lawrence et al. 1985; Kotilainen et al. 1992). The remaining L -band flux may originate from extended stellar emission roughly along the east-west direction, but a quantitative discussion of the origin of the L -band emission is difficult due to the large time variation of the L -band flux (Sharples et al. 1984).

In Fig. 2, a broad absorption-like feature is recognizable at ~ 3.35 – $3.55 \mu\text{m}$. We regard the feature as the 3.4 μm

carbonaceous dust absorption. A continuum level is determined by finding the best fitted line to the data points at $<3.26 \mu\text{m}$ and at 3.58 – $3.72 \mu\text{m}$, as was done for NGC 3094. The adopted continuum level is shown in Fig. 2 as a solid line. The $\tau_{3.4}$ against this continuum level is ~ 0.08 . Any other reasonable continuum levels provide consistent values for $\tau_{3.4}$ within 20%.

In this figure, the presence of the 3.3 μm PAH emission feature is less clear than in the spectrum of NGC 3094. At the redshift of $z = 0.009$, the wavelength of the peak of the 3.3 μm PAH emission feature ($\sim 3.29 \mu\text{m}$ in the rest-frame; Tokunaga et al. 1991) is redshifted to $\sim 3.32 \mu\text{m}$, where the signals are extremely small due to the strong methane absorption by Earth's atmosphere. Hence, it is difficult to quantitatively estimate the 3.3 μm PAH emission flux in this spectrum. We tentatively estimate the rest-frame equivalent width of the 3.3 μm PAH emission as $<1.8 \times 10^{-3} \mu\text{m}$.

It should be noted that Moorwood (1986) reported the detection of the 3.3 μm PAH emission feature with a $7''.5$ aperture, although the significance level of the detection was $<3\sigma$. Moorwood's aperture size is larger than that of Roche et al. (1991; $4''.2$) and of the present data ($1''.2 \times 5''$). The radio map of this galaxy shows extended emission in addition to unresolved emission (Unger et al. 1987). Since the direction of the extended radio emission is roughly in the east-west direction, the same as that of the edge-on host galaxy (Sharples et al. 1984; Anupama et al. 1995), the extended radio emission is thought to originate from star-forming regions in the host galaxy. These star-forming regions could explain the possible detection of the 3.3 μm PAH emission by Moorwood (1986) using a large aperture.

4.3 NGC 7479

A flux-calibrated spectrum of NGC 7479 is shown in Fig. 3. Our data give $L = 10.5$ mag. Nearly all of the L -band flux within a $5''$ aperture ($L = 10.4$ mag; Willner et al. 1985) is detected in the spectrum ($1''.2 \times 5''$ aperture).

An absorption-like feature at ~ 3.35 – $3.55 \mu\text{m}$ is recognizable in the spectrum in Fig. 3. This feature is interpreted as the 3.4 μm carbonaceous dust absorption. A continuum level is determined in the same way as was done for NGC 3094 and NGC 7172. The adopted continuum level is shown in Fig. 3 as a solid line. The $\tau_{3.4}$ against this continuum level is ~ 0.25 .

The presence of the 3.3 μm PAH emission is not clear. The rest-frame equivalent width of the 3.3 μm PAH emission is estimated to be $<7.2 \times 10^{-3} \mu\text{m}$.

5 DISCUSSION

5.1 Relation between the $\tau_{3.4}/\tau_{9.7}$ ratios and the inclination of the host galaxies

In general, emission at $>3 \mu\text{m}$ from the inner few arcsec of (moderately highly-luminous) obscured AGNs is dominated by a compact AGN component and not by extended stellar emission (Alonso-Herrero et al. 1998). In this case, the observed optical depths of dust absorption features reflect the column density of dust in front of a background emission associated with AGN activity.

In the spectrum of NGC 3094, both the $3.4\text{ }\mu\text{m}$ carbonaceous dust absorption and the $3.3\text{ }\mu\text{m}$ PAH emission are detected. Thus, its nuclear $3\text{--}4\text{ }\mu\text{m}$ emission is a composite of a highly obscured AGN and detectable star-forming activity. In this case, the absorption-like feature at $\sim 10\text{ }\mu\text{m}$ is caused not only by the $9.7\text{ }\mu\text{m}$ silicate dust absorption but also by the $7.7\text{ }\mu\text{m}$ PAH emission. The estimate of the column density of carbonaceous dust in front of a background obscured AGN based on the observed $\tau_{3.4}$ value is uncertain because star-forming activity contaminates the $3\text{--}4\text{ }\mu\text{m}$ continuum emission.

In the spectra of NGC 7172 and NGC 7479, the $3.4\text{ }\mu\text{m}$ carbonaceous dust absorption is detected, but no $3.3\text{ }\mu\text{m}$ PAH emission is detected. Hence, their nuclear spectra are thought to be dominated by the emission of highly obscured AGNs. In this case, the absorption-like feature at $\sim 10\text{ }\mu\text{m}$ detected in ground-based $8\text{--}13\text{ }\mu\text{m}$ spectra is ascribed mostly to the $9.7\text{ }\mu\text{m}$ silicate dust absorption. The ground-based $8\text{--}13\text{ }\mu\text{m}$ spectra of Roche et al. (1991) give the optical depths $\tau_{9.7}$ of the $9.7\text{ }\mu\text{m}$ silicate dust absorption feature as >2 and ~ 2.5 , respectively, for NGC 7172 and NGC 7479 (Table 2). Using these $\tau_{9.7}$ values, the ratios $\tau_{3.4}/\tau_{9.7} < 0.04$ and $\tau_{3.4}/\tau_{9.7} \sim 0.10$ are obtained towards the nuclei of NGC 7172 and NGC 7479, respectively. The $\tau_{3.4}/\tau_{9.7}$ ratios are 0.06–0.07 towards any direction in the Galactic diffuse interstellar medium (Pendleton et al. 1994; Roche & Aitken 1984, 1985).

In the literature, we find three more nuclei with detected dust absorption at $3.4\text{ }\mu\text{m}$ and $9.7\text{ }\mu\text{m}$, and no detectable PAH emission features. These three sources, together with NGC 7172 and NGC 7479, are summarized in Table 2. Among the five sources, NGC 7172 and NGC 5506 show $\tau_{3.4}/\tau_{9.7}$ ratios smaller than the ratios in the Galactic diffuse interstellar medium, while NGC 7479, NGC 1068, and IRAS 08572+3915 show larger $\tau_{3.4}/\tau_{9.7}$ ratios.

Since the Galactic extinction is negligible towards all five nuclei ($A_V < 1$ mag; Burstein & Heiles 1984; the Einstein On-Line Service [†]), the dust extinction must be outside the Galaxy. The host galaxies of NGC 7172 and NGC 5506, the two sources with smaller $\tau_{3.4}/\tau_{9.7}$ ratios, are seen from an almost edge-on direction (Sharples et al. 1984; Anupama et al. 1995; Whittle 1992), while the viewing directions towards the host galaxies of NGC 7479, NGC 1068, and IRAS 08572+3915, the three sources with larger $\tau_{3.4}/\tau_{9.7}$ ratios, are relatively face-on (Ma, Peng & Gu 1998; Whittle 1992; Surace et al. 1998). A trend is found, that the $\tau_{3.4}/\tau_{9.7}$ ratios are smaller than the Galactic value in two nuclei with edge-on host galaxies, while the ratios are larger in three nuclei with face-on host galaxies.

We interpret all five nuclei as powered predominantly by obscured AGN activity, based on the absence of detectable PAH emission features at $3\text{--}4\text{ }\mu\text{m}$ and $8\text{--}13\text{ }\mu\text{m}$. However, since the detection feasibility of the PAH emission depends on the spectral quality of individual sources, emission of star-forming activity could be non-negligible in some of the five nuclei. In this case, the $\tau_{3.4}$ value could be suppressed and the apparent $\tau_{9.7}$ value could increase (section 1), that is, the $\tau_{3.4}/\tau_{9.7}$ ratio could decrease. Hence, although the interpretation of smaller $\tau_{3.4}/\tau_{9.7}$ ratios requires some cau-

tions, the larger $\tau_{3.4}/\tau_{9.7}$ ratios cannot be caused by the possible contamination of the emission of star-forming activity.

5.2 Possible explanations for the smaller and larger $\tau_{3.4}/\tau_{9.7}$ ratios

First, smaller $\tau_{3.4}/\tau_{9.7}$ ratios are found towards two highly obscured AGNs whose host galaxies are seen from an edge-on direction. It seems reasonable that dust in the host galaxies are responsible for the obscuration (Young et al. 1996; Murayama, Mouri & Taniguchi 2000). The galaxy types of these host galaxies are S0–Sa (Anupama et al. 1995; Kinney et al. 1991), earlier than that of the Galaxy (Sb/bc; Kerr 1993). If the contribution by carbonaceous dust to dust extinction is smaller in these host galaxies, the smaller $\tau_{3.4}/\tau_{9.7}$ ratios could be explained.

Next, larger $\tau_{3.4}/\tau_{9.7}$ ratios are found in three highly obscured AGNs for which the viewing directions towards their host galaxies are relatively face-on. Carbonaceous dust is more easily destroyed than silicate dust (Draine & Salpeter 1979). If the obscuring dust towards the three AGNs suffers less dust destruction than the Galactic diffuse interstellar medium, then the larger $\tau_{3.4}/\tau_{9.7}$ ratios could be explained. However, we suggest that the larger ratios can be explained more naturally by the presence of a temperature gradient in the obscuring dust. If the obscuring dust is located close to a central compact energy source, a temperature gradient is predicted to occur, with the temperature of the dust decreasing with increasing distance from the central engine (Pier & Krolik 1992). The temperature of the innermost dust (< a few pc) is expected to be ~ 1000 K, close to the dust sublimation temperature. Since emission at $\sim 3\text{ }\mu\text{m}$ is dominated by dust at ~ 1000 K, the extinction estimated using the $\sim 3\text{ }\mu\text{m}$ data (i.e., observed $\tau_{3.4}$) should reflect the value towards the innermost dust around the central energy source. On the other hand, dust at ~ 300 K, a dominant emission source at $10\text{ }\mu\text{m}$, is located further out than the ~ 1000 K dust, and thus the extinction estimated using the $\sim 10\text{ }\mu\text{m}$ data (i.e., observed $\tau_{9.7}$) is only towards the outer region. Hence, the $\tau_{3.4}/\tau_{9.7}$ ratios can be significantly larger. If this suggestion is correct, our results may provide spectroscopic evidence for the presence of the putative “dusty tori” in the close vicinity (< a few pc in inner radius) of AGNs (Antonucci 1993).

6 SUMMARY

The following main results have been found.

- (i) The $3.4\text{ }\mu\text{m}$ carbonaceous dust absorption feature has been detected towards the nuclei of NGC 3094, NGC 7172, and NGC 7479. These nuclei are those with a strong absorption-like feature at $\sim 10\text{ }\mu\text{m}$ but with no detectable PAH emission features in ground-based $8\text{--}13\text{ }\mu\text{m}$ spectra. NGC 3094 shows a detectable $3.3\text{ }\mu\text{m}$ PAH emission feature, while NGC 7172 and NGC 7479 do not. The detection of the $3.4\text{ }\mu\text{m}$ absorption, together with the non-detection of the $3.3\text{ }\mu\text{m}$ PAH emission, suggests that the nuclei of NGC 7172 and NGC 7479 are powered by highly obscured AGN activity. Their strong absorption-like feature at ~ 10

[†] The ftp address is 131.142.11.73.

μm should be attributed mostly to $9.7\ \mu\text{m}$ silicate dust absorption. On the other hand, the detection of both $3.4\ \mu\text{m}$ absorption and $3.3\ \mu\text{m}$ PAH emission in NGC 3094 suggests that the nucleus is powered both by highly obscured AGN activity and detectable star-forming activity. Both the $9.7\ \mu\text{m}$ silicate dust absorption and the $7.7\ \mu\text{m}$ PAH emission could be responsible for the strong absorption-like feature at $\sim 10\ \mu\text{m}$.

(ii) We compared the $\tau_{3.4}/\tau_{9.7}$ ratios for five highly obscured AGNs with detected $3.4\ \mu\text{m}$ and $9.7\ \mu\text{m}$ absorption and without detectable PAH emission features. We found that the ratios in the three highly obscured AGNs whose host galaxies are seen from a face-on direction are larger than the ratios in the Galactic diffuse inter-stellar medium or the ratios in the two highly obscured AGNs whose host galaxies are seen from an edge-on direction. For the three sources, the larger ratios can be explained if the obscuring dust is so close to the central AGNs that a temperature gradient occurs in it. Our results may provide spectroscopic evidence for the presence of the putative "dusty tori" around AGNs.

ACKNOWLEDGMENTS

We thank Dr. T. Kerr, Dr. J. Davies, T. Carroll, and T. Wold for their support during the UKIRT observing run, and Dr. C. C. Dudley for his careful reading of the manuscript. L. Good kindly proofread this manuscript. The anonymous referee gave useful comments. The United Kingdom Infrared Telescope is operated by the Joint Astronomy Centre on behalf of the U.K. Particle Physics and Astronomy Research Council. Drs. A. T. Tokunaga and H. Ando give MI the opportunity to work at the University of Hawaii. MI is financially supported by the Japan Society for the Promotion of Science during his stay at the University of Hawaii.

REFERENCES

Aitken D. K., Jones B., 1973, *ApJ*, 184, 127
 Allamandola L. J., Tielens A. G. G. M., Barker J. R., 1989, *ApJS*, 71, 733
 Alonso-Herrero A., Simpson C., Ward M. J., Wilson A. S., 1998, *ApJ*, 495, 196
 Antonucci R., 1993, *ARA&A*, 31, 473
 Anupama G. C., Kembhavi A. K., Elvis M., Edelson R., 1995, *MNRAS*, 276, 125
 Armus L., Heckman T. M., Miley G. K., 1989, *ApJ*, 347, 727
 Bridger A., Wright C. S., Geballe T. R., 1994, in McLean I., ed., *Infrared Astronomy with Arrays: The Next Generation*, Kluwer, Dordrecht, p. 537
 Burstein D., Heiles C., 1984, *ApJS*, 54, 33
 Clavel J., Schulz B., Altieri B., Barr P., Claes P., Heras A., Leech K., 1999, in Gaskell C. M., Brandt W. N., Dietrich M., Dultzin-Hacyan D., Eracleous M., eds., *ASP Conf. Ser.* 175, *Structure and Kinematics of Quasar Broad Line Regions*. Astron. Soc. Pac., San Francisco, p. 387 (*astro-ph/9806054*)
 Draine B. T., Salpeter E. E., 1979, *ApJ*, 231, 438
 Dudley C. C., 1998, PhD thesis, University of Hawaii
 Dudley C. C., 1999, *MNRAS*, 307, 553
 Dudley C. C., Wynn-Williams C. G., 1997, *ApJ*, 488, 720
 Genzel R., et al., 1998, *ApJ*, 498, 579
 Glass I. S., Moorwood A. F. M., 1985, *MNRAS*, 214, 429
 Ho L. C., Filippenko A. V., Sargent W. L. W., 1997, *ApJS*, 112, 315
 Huang J. H., Gu Q. S., Su H. J., Hawarden T. G., Liao X. H., Wu G. X., 1996, *A&A*, 313, 13
 Imanishi M., 2000, *MNRAS*, 313, 165
 Imanishi M., Terada H., Sugiyama K., Motohara K., Goto M., Maihara T., 1997, *PASJ*, 49, 69
 Kerr F. J., 1993, in Holt S. S., Verter F., eds., *AIP Conf. Proc.* 278, *Back to the Galaxy*, AIP, New York, p. 3
 Kinney A. L., Antonucci R. R. J., Ward M. J., Wilson A. S., Whittle M., 1991, *ApJ*, 377, 100
 Kotilainen J. K., Ward M. J., Boisson C., Depoy D. L., Bryant L. R., Smith M. G., 1992, *MNRAS*, 256, 125
 Larkin J. E., Armus L., Knop R. A., Soifer B. T., Matthews K., 1998, *ApJS*, 114, 59
 Lawrence A., Ward M., Elvis M., Fabbiano G., Willner S. P., Carleton N. P., Longmore A., 1985, *ApJ*, 291, 117
 Ma J., Peng Q. -H., Gu Q. -S., 1998, *A&AS*, 130, 449
 Moorwood A. F. M., 1986, *A&A*, 166, 4
 Mountain C. M., Robertson D. J., Lee T. J., Wade R., 1990, *Proc. SPIE*, 1235, 25
 Murayama T., Mouri H., Taniguchi Y., 2000, *ApJ*, 528, 179
 Pendleton Y. J., 1996, in Greenberg J., ed., *The Cosmic Dust Connection*, Kluwer, Dordrecht, p. 71
 Pendleton Y. J., Sandford S. A., Allamandola L. J., Tielens A. G. G. M., Sellgren K., 1994, *ApJ*, 437, 683
 Piccinotti G., Mushotzky R. F., Boldt E. A., Holt S. S., Marshall F. E., Serlemitsos P. J., Shafer R. A., 1982, *ApJ*, 253, 485
 Pier E. A., Krolik J. H., 1992, *ApJ*, 401, 99
 Rigopoulou D., Spoon H. W. W., Genzel R., Lutz D., Moorwood A. F. M., Tran Q. D., 1999, *AJ*, 118, 2625
 Roche P. F., Aitken D. K., 1984, *MNRAS*, 208, 481
 Roche P. F., Aitken D. K., 1985, *MNRAS*, 215, 425
 Roche P. F., Aitken D. K., Phillips M. M., Whitmore B., 1984, *MNRAS*, 207, 35
 Roche P. F., Aitken D. K., Smith C. H., Ward M. J., 1991, *MNRAS*, 1991, 248, 606
 Sandage A., Tammann G. A., 1987, *A Revised Shapley-Ames Catalog of Bright Galaxies*, Carnegie Institution of Washington Publication 635, Washington, D. C., Second Edition, p. 66
 Sharples R. M., Longmore A. J., Hawarden T. G., Carter D., 1984, *MNRAS*, 208, 15
 Smith R. G., Sellgren K., Brooke T. Y., 1993, *MNRAS*, 263, 749
 Surace J. A., Sanders D. B., Vacca, W. D., Veilleux S., Mazzarella, J. M., 1998, *ApJ*, 492, 116
 Tokunaga A. T., Sellgren K., Smith R. G., Nagata T., Sakata A., Nakada Y., 1991, *ApJ*, 380, 452
 Unger S. W., Lawrence A., Wilson A. S., Elvis M., Wright A. E., 1987, *MNRAS*, 228, 521
 Whittle M., 1992, *ApJS*, 79, 49
 Willner S. P., Elvis M., Fabbiano G., Lawrence A., Ward M. J., 1985, *ApJ*, 299, 443
 Wright G. S., Bridger A., Geballe T. R., Pendleton Y., 1996, Block D. L., & Greenberg J. M., (eds), in *New Extragalactic Perspectives in the New South Africa*, Dordrecht, Kluwer, p.143
 Young S., Hough J. H., Efstatithiou A., Wills B. J., Bailey J. A., Ward M. J., Axon D. J., 1996, *MNRAS*, 281, 1206

Table 1. Observing log

Object	z	Date (UT)	Integration Time (sec)	Air Mass	Name	Standard Star		
						L -mag	Type	Temperature (K)
NGC 3094	0.008	Feb 21, 2000	2560	1.0–1.2	HR 3975	3.3	A0Ib	9700
NGC 7172	0.009	Sep 9, 1999	3200	1.6–1.7	HR 8087	5.3	A0V	9480
NGC 7479	0.008	Sep 9, 1999	2400	1.0–1.1	HR 8911	4.9	A0	9480

Table 2. The $\tau_{3.4}$, $\tau_{9.7}$ and $\tau_{3.4}/\tau_{9.7}$ towards sources with detected $3.4\ \mu\text{m}$ and $9.7\ \mu\text{m}$ absorption features and with no detectable PAH emission features.

Object	z	$\tau_{3.4}$	$\tau_{9.7}$	$\tau_{3.4}/\tau_{9.7}$	References
NGC 1068	0.004	0.12	0.52	0.23	1, 2
IRAS 08572+3915	0.058	0.9	5.2	0.17	3, 4
NGC 7479	0.008	0.25	~ 2.5	0.10	5, 6
NGC 5506	0.006	0.03	1.3	0.02	7, 2
NGC 7172	0.009	0.08	> 2	< 0.04	5, 6

References. — (1) Imanishi et al. 1997; (2) Roche et al. 1984; (3) Pendleton 1996; (4) Dudley & Wynn-Williams 1997; (5) this work; (6) estimated based on the spectra of Roche et al. (1991). We estimate $\tau_{9.7}$ by (a) using the formula of $\tau_{9.7} = \ln \left[\frac{F_\lambda(8) + F_\lambda(13)}{2F_\lambda(9.7)} \right]$ (Aitken & Jones 1973), and by (b) deriving the optical depth at $9\ \mu\text{m}$ (τ_9) and by adopting the relation of $\tau_{9.7}/\tau_9 \sim 1.7$ (Dudley & Wynn-Williams 1997). Both methods provide consistent results; (7) Imanishi 2000.

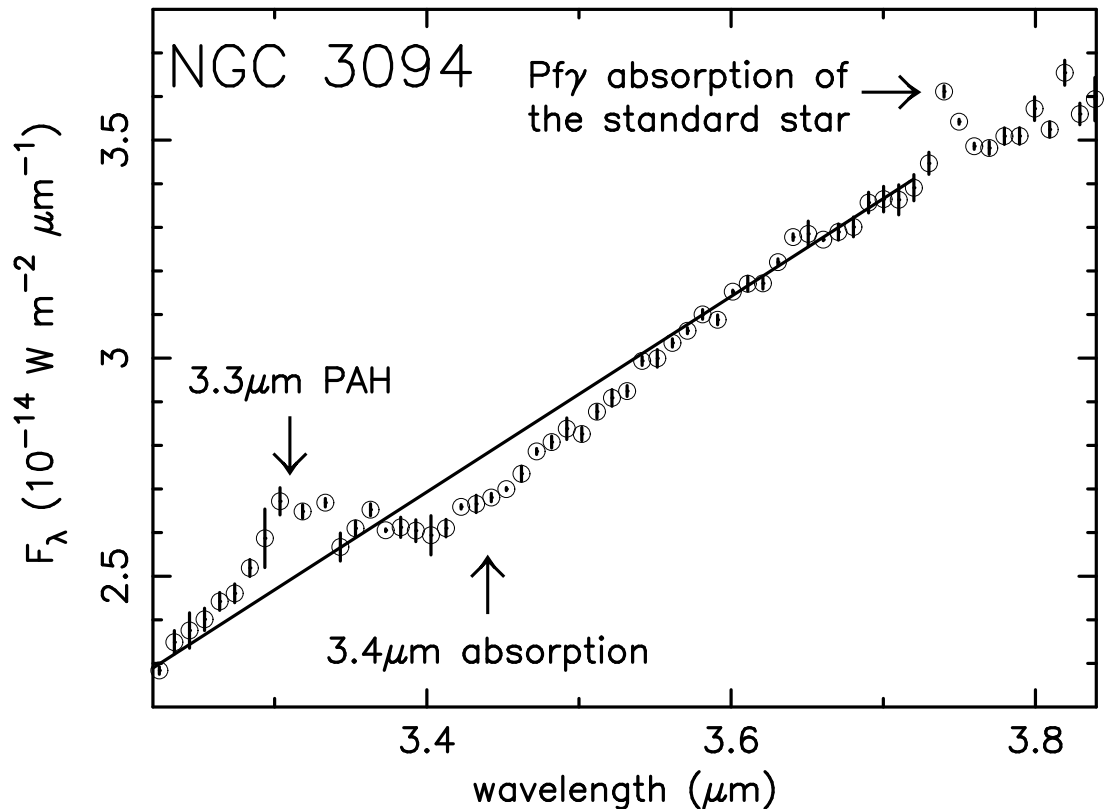


Figure 1. A flux-calibrated spectrum of NGC 3094. A spectral resolution is ~ 350 after binning. The ordinate is F_λ in $\text{W m}^{-2} \mu\text{m}^{-1}$, and the abscissa is the observed wavelength in μm . The solid line is the adopted continuum level to measure the optical depth of the $3.4 \mu\text{m}$ absorption feature (see text). The emission-like feature at $3.74 \mu\text{m}$ is caused by the stellar absorption of the type-A standard star (see text).

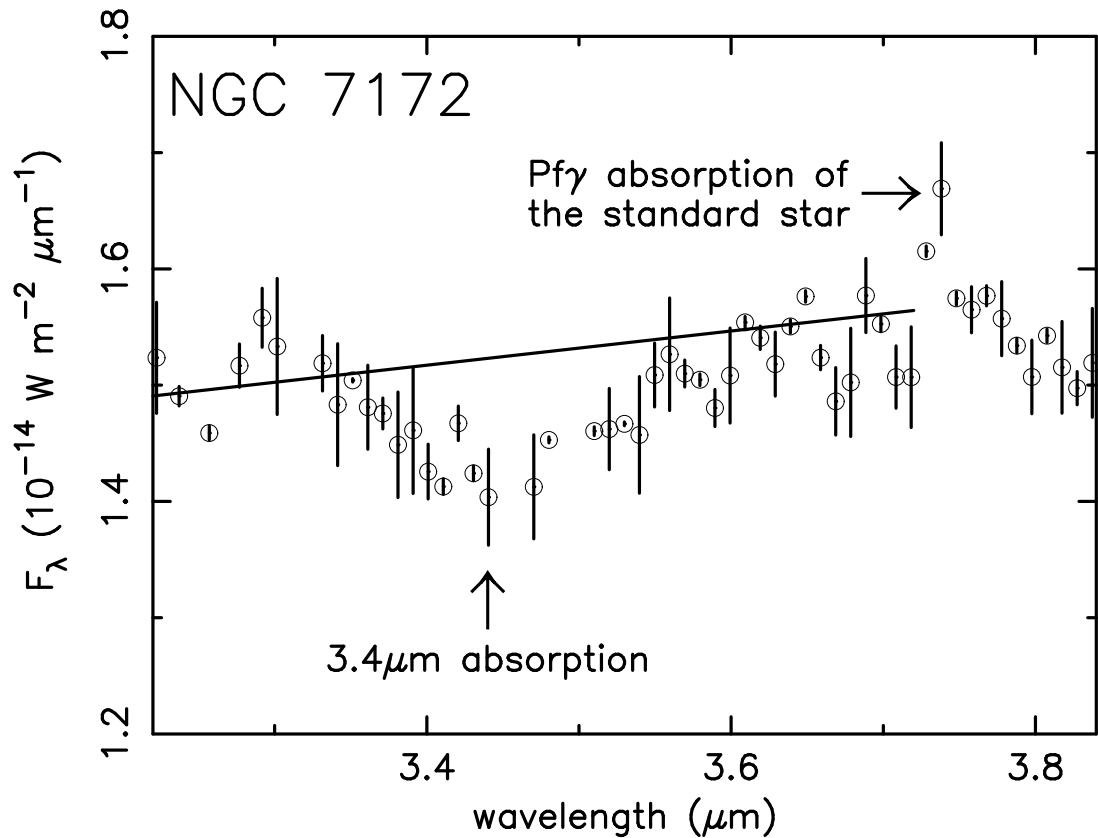


Figure 2. A flux-calibrated spectrum of NGC 7172, displayed in the same way as NGC 3094 (Fig. 1).

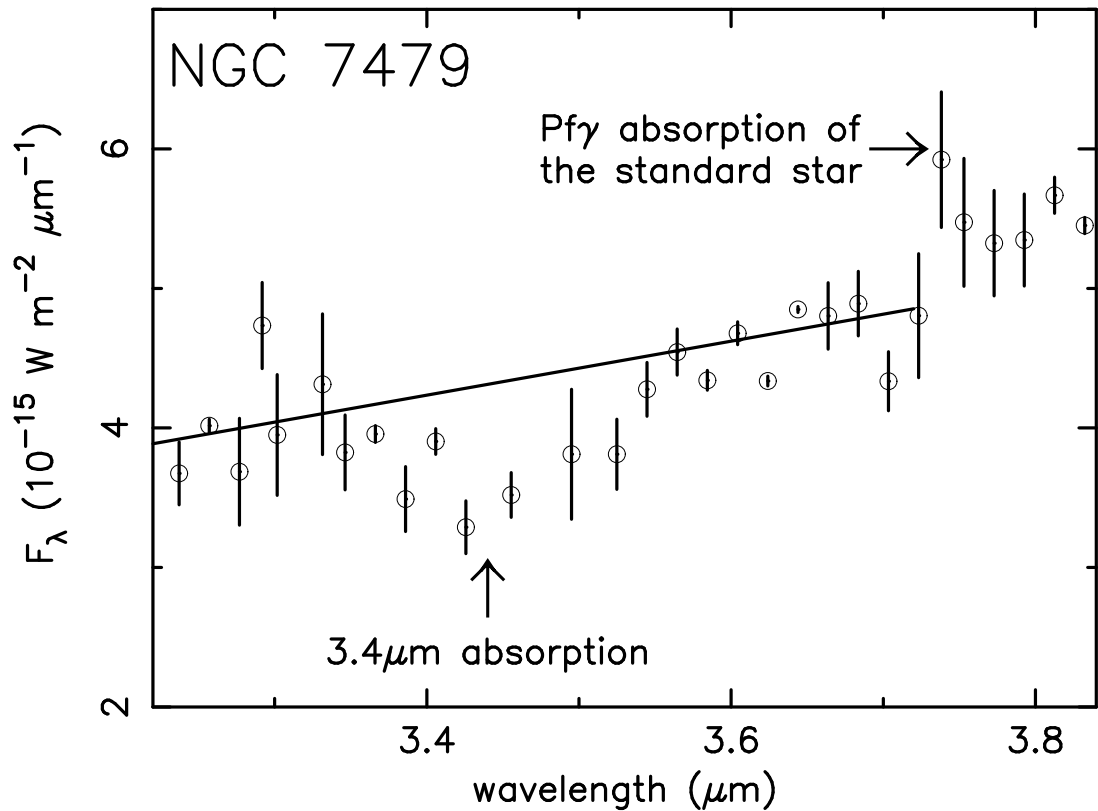


Figure 3. A flux-calibrated spectrum of NGC 7479, displayed in the same way as NGC 3094 (Fig. 1). This spectrum is shown with a spectral resolution of ~ 170 at $3.5 \mu\text{m}$.